

NEAR-INFRARED 0".15 RESOLUTION IMAGING OF THE GALACTIC CENTER

A. ECKART, R. GENZEL, R. HOFMANN, B. J. SAMS, AND L. E. TACCONI-GARMAN
 Max-Planck-Institut für extraterrestrische Physik, Giessenbachstrasse, W-8046 Garching bei München, Germany

Received 1993 January 11; accepted 1993 February 10

ABSTRACT

We present deep 1.6 (*H*) and 2.2 μm (*K*) images of the central parsec of the Galaxy at a resolution of 0".15. Most of the flux in earlier seeing-limited images comes from about 340 unresolved stellar sources with *K*-magnitudes ≤ 14 . Most of the fainter stars in the central parsec are likely M- rather than K-giants. The IRS 16 and 13 complexes are resolved into about 25 and six sources, a number of which are probably luminous hot stars. We confirm the presence of a blue near-infrared object ($K \approx 13$) at the position of the compact radio source Sgr A*. The spatial centroid of the number distribution of compact sources is consistent with the position of Sgr A* but not with a position in the IRS 16 complex. The stellar surface density is very well fitted by an isothermal cluster model with a core radius of 0.15 ± 0.05 pc. The central stellar density is close to $10^8 M_{\odot} \text{pc}^{-3}$. Buildup of massive stars by collisional merging of lower mass stars and collisional disruption of giant atmospheres are very probable processes in the central 0.2 pc.

Subject headings: galaxies: nuclei — Galaxy: center — infrared: stars

1. INTRODUCTION

The nature of the stellar cluster in the Galactic center has been subject of many investigations (e.g., Bailey 1980; Allen 1987) ever since the first near-infrared mapping of Becklin & Neugebauer (1968). Here we report initial results of 0".15 resolution (6.2×10^{-3} pc at 8.5 kpc) near-infrared images of the central parsec which expand on Eckart et al. (1992). A more detailed discussion is in preparation.

2. OBSERVATION AND DATA REDUCTION

We employed the new MPE infrared high-resolution camera, SHARP (Hofmann et al. 1993), at the New Technology Telescope (NTT) of the European Southern Observatory (ESO) in La Silla, Chile, for near-diffraction limited imaging at *H* (1.6 μm) and *K* (2.2 μm) of the central $\approx 10''$ radius region. The observations were carried out in 1992 March 22–25 (*K*) and 1992 August 11 (*H*). The image scale was 0".05 pixel $^{-1}$, and integration times were 0.3–1 s per frame. The individual frames were dead pixel corrected, flat-fielded, and a simple shift-and-add (SA) algorithm (e.g., Christou 1991) was applied to seeing-selected images. The long-exposure seeing was between 0".8 and 1".0 FWHM. The short-exposure seeing varied between 0".3 and 0".5 FWHM, and the bright SA reference sources (IRS 7 or IRS 16NE) were dominated by a single, bright speckle. Our field of view was always well within the near infrared isoplanatic patch. Figure 1 (bottom right) shows that the resulting co-added SA images consist of 0".15 FWHM diffraction-limited images of the objects on top of a seeing background starting at the 30% peak intensity level. To remove this seeing background the images were "CLEANed" with their extracted average SA reference point-spread function (IRS 7 or IRS 16NE) and/or a point-spread function of a nearby reference star (usually 9 Sgr) using a Lucy algorithm (Lucy 1974). The CLEANed images were then reconvolved with a Gaussian of 0".15 FWHM. Earlier speckle image reconstruction using the Knox-Thompson method (Knox 1976) gave very similar results (Eckart et al. 1992; see also Eckart & Duhoux 1990). For the Galactic center (a crowded field of compact sources with a flux range of $> 10^3$) and data taken under excellent seeing conditions the nonlinear, flux-conserving Lucy algorithm has proved to be straightforward

and successful in reaching high dynamic range and high spatial resolution.

3. RESULTS AND DISCUSSION

Figure 1 shows a mosaic of *K*-band image reconstructions of the central cluster. Figure 2 (Plate 3) is a false color representation of the same data. For the central part of the image (upper right insets of Figs. 1 and 2) the total integration time is ≈ 4 hr (30,000 frames). With the exception of a source about 2" S of the compact Sgr A* radio source the image agrees very well with and significantly improves that of Eckart et al. (1992). Our new data are also in good agreement with earlier observations by DePoy & Sharp (1991: resolution of 0".9; enhanced 0".4) and the 0".01 resolution lunar occultation measurements by Simon et al. (1990) and Simons, Hodapp, & Becklin (1990). The faintest sources reliably detected have a *K*-band magnitude of 14, implying a dynamic range of more than 7 mag with respect to IRS 7 ($K = 6.8$). The *H*-band image used for the *H*–*K* color map in Figure 2 contains 4000 frames, has a resolution of 0".3 and a limiting magnitude of 15.

3.1. The Cluster Is Resolved into Individual Stars

The *K*-band emission from the central parsec is resolved into individual stars and groups of stars. There is no convincing evidence for extended/diffuse 2 μm emission, or a bright central cusp. Several examples of complex emission structures—probably due to local crowding of stars—are evident (e.g., the IRS 13 area and a 1".5 NS ridge south of Sgr A*). Within the flux density calibration uncertainties (less than 10% for our data) the speckle image with 340 compact sources of $K \leq 14$ contains *all* the flux density reported in earlier seeing-limited images (Fig. 3), two-thirds of it in the brightest 29 sources ($K < 10.5$). Comparison of our speckle and long exposure images shows that apparent diffuse emission in $\geq 1''$ resolution images is due to a combination of smearing of faint sources and wings of the point-spread functions of bright sources. The central IRS 16 complex now splits up into about 25 sources. Lunar occultation observations show that the brightest of these are likely single or multiple stars (but not large clusters), as their sizes are less than 100 AU (Simon et al. 1990; Simons et al. 1990). The extended ridge in IRS 16SW-E found by other authors (DePoy & Sharp 1991;

PLATE L3

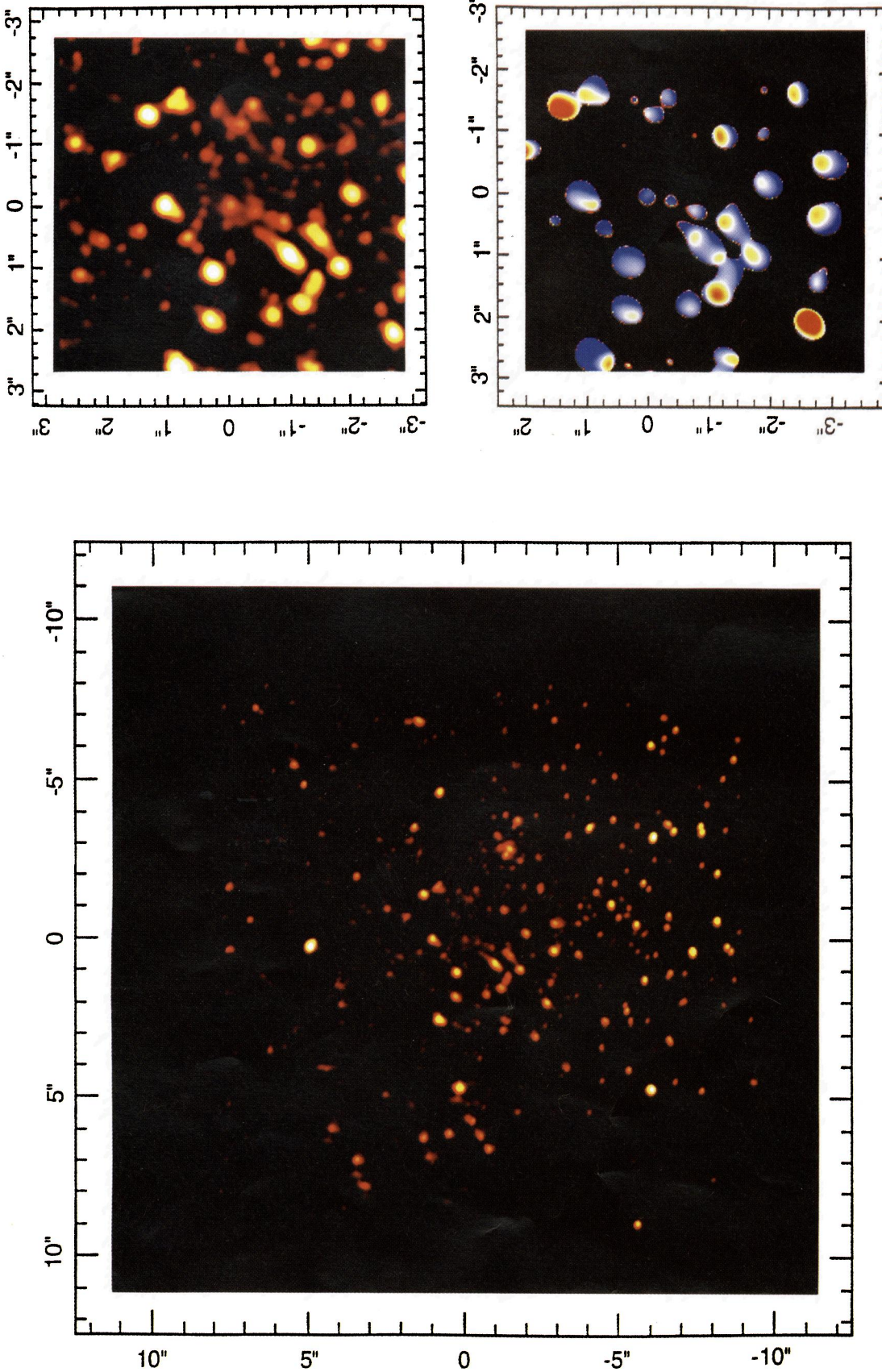


FIG. 2.—*Left*: False color representation of the speckle image reconstruction for $K \leq 14.5$ sources in the central $20'' \times 20''$. The spatial resolution is $0''.15$ FWHM. Offsets are from the strongest (western) component of the infrared counterpart of Sgr A*. *Top right*: false color map of $K \leq 15$ sources in the most sensitive central $6''.4 \times 6''.4$ of the Galactic center region. The spatial resolution is $0''.15$ FWHM. *Bottom right*: $H - K$ color map of the central $6''.4 \times 6''.4$ of the Galactic center region. The map was obtained by aligning the K - and H -band maps on a subpixel level and matching their spatial resolutions to $0''.3$. Blue colors correspond to λ^{-2} spectra ($H - K \approx 0.0$ with $A_K = 3.4$, $A_H = 5.4$, Rieke et al. 1989). Red colors ($H - K \approx 1.0$) correspond to flat spectra. The H -band image used for the $H - K$ color map in Fig. 2 contains 4000 frames and has a resolution of $0''.3$ and limiting magnitude of 15.

ECKART et al. (see 407, L77)

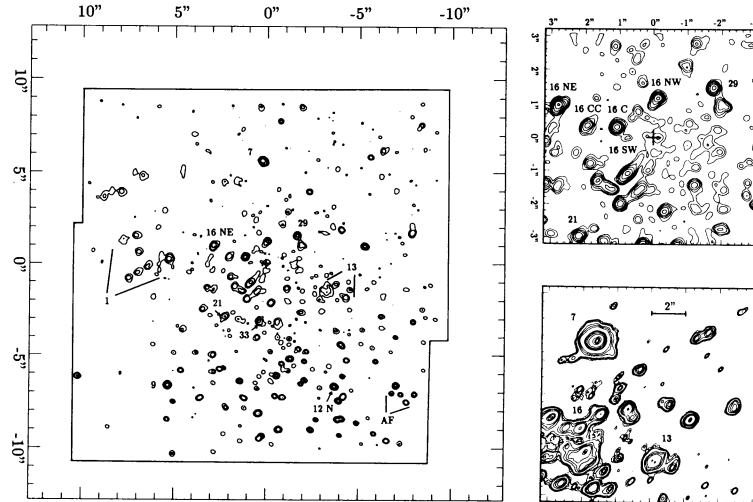


FIG. 1.—*Left*: Mosaic of K -band speckle image reconstructions of the central $20'' \times 20''$ of the Galaxy at a spatial resolution of $0''.15$ FWHM centered on the position of the compact radio source Sgr A* (cross). Boundaries of the mosaic are indicated by solid lines. Contour levels are 14.5, 12.5, 10.5, 8.5, 6.8 mag. Faint sources within a radius of $1''.5$ of IRS 7 may be missing. Three different techniques were combined for registration of Sgr A*: (1) Positioning our K -band sources from their observed offsets from IRS 7 and its known absolute position (Becklin et al. 1987). (2) Offsets of Sgr A* from IRS 7 were derived from recent radio maps showing both Sgr A* and the ionized tail of IRS 7 (Yusef-Zadeh & Melia 1992). (3) Relative positions were obtained from a comparison of radio continuum and NIR recombination line maps (Forrest et al. 1987; W. Forrest 1992, private communication; Krabbe et al. 1993). The average position from (1) \rightarrow (3) and its estimated systematic uncertainty ($\pm 0''.2$) are shown in Fig. 1 and agree well with other results (Tollestrup, Capps, & Becklin 1989; DePoy & Sharp 1991; Rosa et al. 1991; Forrest et al. 1987; Rieke et al. 1989). *Top right*: K -band contour map of the central $6''.4 \times 6''.4$ of the Galactic center region centered on the position of the compact radio source Sgr A* (cross). This most sensitive part of the image contains information of about 30,000 individual frames taken with integration times between 0.3 and 1.0 s each. The spatial resolution is $0''.15$ FWHM. Contour levels are 15, 14, ..., 9 mag. *Bottom right*: Raw shift-and-add image of a representative subset of 3000 K -band frames. Contour levels are 0.2%, 0.25%, 0.3%, 0.5%, 0.7%, 1%, 3%, 4%, 6%, 10%, 30%, 50%, 70%, 100% of the peak intensity of IRS 7 ($K = 6.8$).

Simon et al. 1990) is resolved into at least five stellar sources. IRS 13 is resolved into a $\approx 0''.5$ radius cluster with at least five to 10 members.

3.2. Derived Properties of the Stellar Cluster

It is now possible to determine a core radius and a central stellar density from the *surface density distribution* assuming that stars emitting at $2 \mu\text{m}$ sample the distribution of the entire cluster. Since the Galactic center contains stars with very different intrinsic fluxes, this method is obviously preferable to the evaluation of the infrared brightness distribution.

Centroid Position and Core Radius. With the possible exception of the IRS 13 complex, there is no compelling evidence for

subclustering in the field. The two-dimensional autocorrelation function of the source positions shows no preferred scales other than the radius of the cluster itself. The IRS 16 complex $\sim 1''$ east of Sgr A* appears to be a group of bright ($K < 11$) stars and not the cusp of the cluster. The spatial median of the source number distribution is $0''.6 \pm 0''.7$ west and $1''.3 \pm 1''.0$ south of Sgr A* (3σ errors). This means that the position of the cluster center could be Sgr A* but *cannot be* substantially further east, in the IRS 16 complex. In contrast the centroid of the $2 \mu\text{m}$ flux density distribution is located on IRS 16. However, for radii up to $10''$ flux-based estimates of the centroid are biased by the high brightness of the IRS 16 sources. On larger scales the flux distribution is significantly affected by

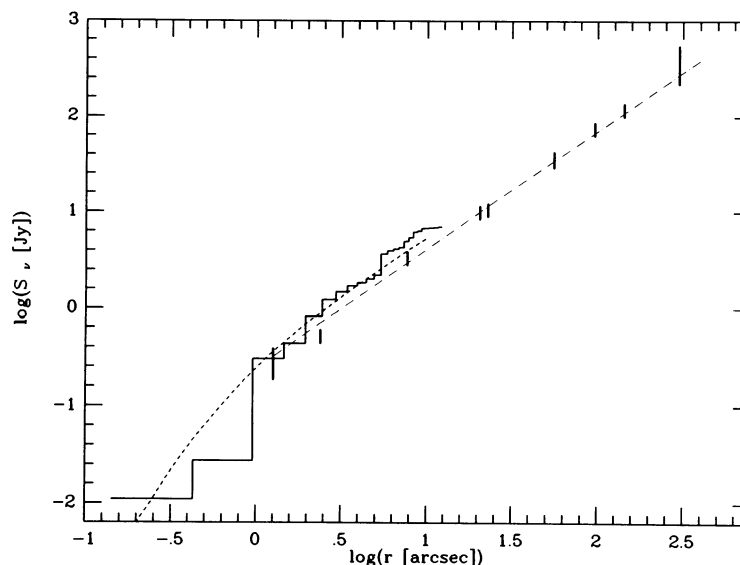


FIG. 3.—Observed K -band flux density S_v in Jy contained in circular apertures of radius r centered on the position of Sgr A* for both the speckle mosaic (solid line histogram) and the long exposure mosaic ($1''$ resolution, short dashed line). The long-dashed line shows a fit to previous data from Becklin & Neugebauer (1968, 1975) as summarized in Bailey (1980) and indicated by thick vertical. Two-thirds of the $2 \mu\text{m}$ continuum flux density in the central $20'' \times 20''$ is contained in the brightest 29 sources with $K < 10.5$.

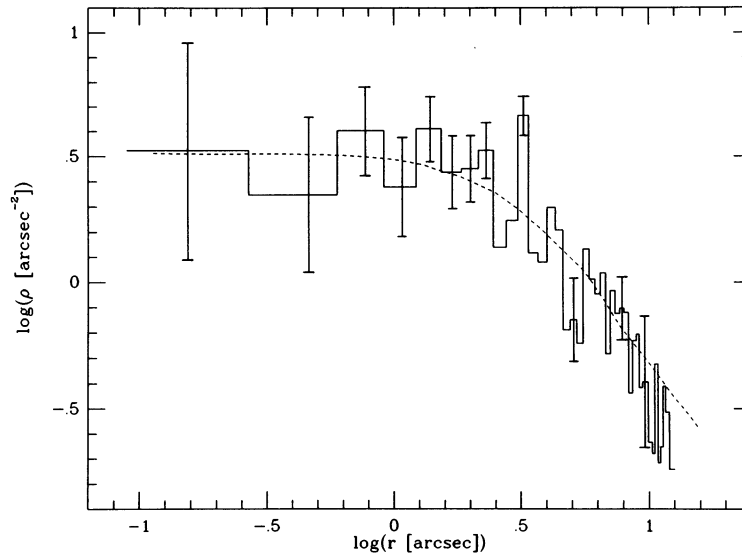


FIG. 4.—Surface density ρ in sources per (arcsec)² for all 340 stars with $K < 14$ in 0".3 wide annuli of radius r from the radio position of Sgr A* (histogram). Representative error bars indicate the statistical ($N^{1/2}$) uncertainties. Note that the data outside 10" have been corrected for incomplete area coverage and the number of sources is small there. The resulting distribution is very well fitted by an isothermal stellar density distribution (dashed curve) with a core radius of 3".8 (0.15 pc) and a central surface density of three sources per (arcsec)².

spatially variable extinction, caused by the circumnuclear gas ring west of Sgr A* (Gatley et al 1989; Genzel 1989). We therefore regard the determination of a centroid from the number distribution in the densest part of the cluster as more reliable. The resulting stellar surface density distribution (Fig. 4) is very well fitted by an isothermal cluster model of core radius $3".8 \pm 1".3$ (0.15 ± 0.05 pc) and central surface density three sources per (arcsec)². A smaller core radius is only possible if there is a several arcsec diameter central region of large NIR extinction (see § 3.4).

The $r^{-1.8}$ volume density power law previously determined from the surface brightness distribution (e.g., Bailey 1980) does not fit the data inside of a few arcseconds. Varying the assumed centroid position anywhere from 1".5 SW of Sgr A* (the formal centroid) to 1" E of Sgr A*, or choosing a cutoff at $K = 13$ instead of 14 varies the derived core radius over the range from 0.1 to 0.2 pc and the central surface density from 2 to 3.3 sources per (arcsec)². The brightest sources ($K \leq 11$) perhaps have a slightly smaller core radius (0.1 pc) than the fainter sources (0.17–0.25 pc). With a core radius of $r_0 = 0.15 \pm 0.05$ pc and a line-of-sight central velocity dispersion $\sigma_0 = 100 \pm 25$ km s⁻¹ (e.g., Sellgren et al. 1990) the central density of the cluster becomes $\rho_0 = 9\sigma_0^2/4\pi Gr_0^2 = 10^{7.9 \pm 0.5} M_\odot \text{pc}^{-3}$, with a core mass of $M_0(r_0) = 10^{5.7 \pm 0.3} M_\odot$.

Sgr A* itself appears to be located in a 2" diameter region of high source density that is itself void of bright stars yet surrounded by them. It is not clear whether the lack of bright stars near Sgr A* signifies an actual lack of those stars, or local extinction, as proposed by Zylka, Mezger, & Lesch (1992). The presence of this "ring" of bright sources around Sgr A* substantially weakens the argument (e.g., Ozernoy 1987; Sanders 1992) that Sgr A* cannot be a very massive object because it is displaced from the apparent centroid of the mass (assumed to be IRS 16).

H–K Colors. Most of the IRS 16 complex are relatively blue as shown in our H–K color image of the central 6".4 and 0".3 resolution (Fig. 2, bottom right). Their dereddened 1.6–2.2 μm spectra follow the λ^{-2} Rayleigh-Jeans law. Several sources (IRS 1W, 13, 21, 29) are significantly redder (see also DePoy & Sharp 1991). These red colors may be due to local extinction by material in the radio mini-spiral (the bar). The individual

source colors across IRS 16SW clearly explain the color gradient noted by DePoy & Sharp (1991).

Blue Supergiants and Red Giants. Figure 2 confirms previous results that the central few arcseconds contain ~ 20 hot stars dominating the 1–2 μm flux density. Given their K -magnitudes (≤ 10.8) these stars must be fairly luminous ($L \geq 10^5 L_\odot$) and probably short-lived. Several of them exhibit strong and broad Br γ , Br α , and He I line emission indicative of dense, fast winds (Forrest et al. 1987; Allen, Hyland, & Hillier 1990; Geballe et al. 1991; Krabbe et al. 1991, 1993). They may be $T \geq 30,000$ K blue supergiants or Wolf-Rayet stars with masses $\geq 30 M_\odot$.

Becklin & Neugebauer (1986) assumed that most of the 2 μm continuum emission is due to K5-giants of about 4000 K color temperature. However, K-giants would have $K \approx 14$ in the Galactic center while most of the fainter sources in the speckle image have $K \approx 11$ –13. Most of the late-type stars in the central parsec are thus more likely M-giants [$K(M3) = 12.5$, $K(M5) = 10.8$] of surface temperature ≈ 3000 K, consistent with the 2 μm CO bandhead spectroscopy of the brightest late-type stars by Sellgren et al. (1987) and Lebofsky, Rieke, & Tokunaga (1982). The higher color temperature derived from large beam near-infrared flux densities may be heavily influenced by the luminous early-type stars discussed above. The lack of CO bandhead absorption toward the central 10" reported by Sellgren et al. (1990) is then a likely consequence of the extra flux of these bright, hot, and massive stars.

3.3. Star Formation and Evolution of the Central Cluster

What are the hot stars in the central parsec and how have they formed? The first possibility is gravitational contraction of dense interstellar clouds possibly aided by collisions and shock compression of clouds. However, at present there is no compelling evidence for self-gravitating gas clouds in the central few parsecs (e.g., Jackson et al. 1993). Perhaps the amount of very dense gas in the innermost region was much greater in the past than it is now, and star formation may be time dependent (e.g., Rieke & Lebofsky 1982).

One key result of the present study is the very high stellar density (10^7 – $10^8 M_\odot \text{pc}^{-3}$) in the core. This environment allows a second possibility for the formation of the hot, massive stars: sequential buildup by collisions and mergers

(Lee 1987, 1990). The time between collisions/merging of two solar mass stars in such an environment is a few 10^9 yr, and the overall collision rate is in excess of 10^{-4} yr $^{-1}$ (Phinney 1989). Calculations including mergers and stellar evolution for such parameters suggest that collisional processes could be an attractive mechanism for explaining the presence of about 10 to 10^2 stars with masses greater than $10 M_{\odot}$ (Lee 1987). Consistent with this hypothesis, all of the hot He I emission-line stars discovered so far by Krabbe et al. (1991, 1993) are located in the dense part of the cluster at $r < 0.5$ pc. If collisional processes create massive stars it would appear almost inevitable that eventually a massive central black hole forms. However, that process may be prevented if stellar winds and supernovae remove sufficient mass, as could be indicated by the winds of the He I stars. Note that the lack of a stellar cusp in the Galactic center does not exclude the presence of a massive black hole if collisional effects are important (Murphy, Cohn, & Durisen 1988).

An alternative possibility is that the identification of the hot stars as massive post-main-sequence stars is not correct. Morris (1993) argues that the hot stars could be $\approx 10 M_{\odot}$ black holes surrounded by an atmosphere acquired in collisions with red giants. However, the proposed compact cluster of a few 10^5 $10 M_{\odot}$ black holes would probably be unstable to formation of a single massive black hole (Goodman & Lee 1989). Clearly a detailed calculation is needed to test whether the atmosphere of a $10 M_{\odot}$ black hole would mimic a He-rich, symmetric wind of expansion velocity 500–1000 km s $^{-1}$ and P Cygni absorption features as seen in the Galactic center He I emission-line stars (Geballe et al. 1991; Krabbe et al. 1993). The spectral characteristics of the brightest He I star (the AF star, Fig. 1) are in fact remarkably similar to those of other He I stars in the Galaxy, including a star recently found in the so called “quintuplet” cluster (Okuda et al. 1990), about 10' (25 pc) north of Sgr A* (Moneti, Glass, & Moorwood 1991; Krenz et al. 1993).

3.4. Sagittarius A*

In agreement with Eckart et al. (1992), we find a $K \approx 13$ source centered within $0''.15$ of the best Sgr A* position that is

already evident in subsets of the raw SA data (Fig. 1). The source either has a $\sim 0''.5$ east-west size or it is multiple with its western component closest to Sgr A*. From the absolute position of Sgr A* (R.A. = $17^{\text{h}}42^{\text{m}}29^{\text{s}}.316$, Decl. = $-28^{\circ}59'18''.38$ [1950], Rosa et al. 1992), we derive the absolute position for the western infrared source as R.A. = $17^{\text{h}}42^{\text{m}}29^{\text{s}}.306$ ($\pm 0''.015$), Decl. = $-28^{\circ}59'18''.45$ ($\pm 0''.2$) (1950). It appears to be part of a $1''.5$ emission ridge (P.A. $\approx -20^{\circ}$). Integrating over $0''.5$ it has $K = 12 \pm 0.5$ and $H = 13.9 \pm 0.5$. With $A_K = 3.4$ and $A_H = 5.4$ (Rieke, Rieke, & Paul 1989) it has a blue color ($H - K \approx 0.0$) similar to other hot sources in the field (Fig. 2, bottom right). The luminosity of the Sgr A* source then is $1-5 \times 10^5$ ($T_{\text{eff}}/35,000 \text{ K}$) $^3 L_{\odot}$, not including possible local extinction. An identification of the new source as the NIR counterpart of Sgr A* can only be tentative at present, as spectroscopic, polarimetric, and proper motion studies are required. The probability of a chance alignment in the crowded central few arcsecs is between 4% and 20%. The submillimeter excess at the position of Sgr A* (Zylka et al. 1992; Serabyn, Carlstrom, & Scoville 1992) could imply a large amount of extinction ($A_V \approx 1000$) toward the central arcsecond if most of the flux is thermal. This could explain the apparent void of bright sources in which Sgr A* is located. The blue color then implies either that the K-band counterpart of Sgr A* is a chance alignment, hot foreground cluster member, or the scattered radiation from a hot accretion disk around Sgr A*. Alternatively the submillimeter excess may be due to a compact ($\approx 10^{12}$ cm) nonthermal component that is self-absorbed at cm- and mm-wavelengths.

We thank W. Forrest for communicating offsets between near-infrared sources and Sgr A*, H. Zinnecker and M. R. Rosa for communicating their high-quality K-band image prior to publication, and A. Harris, P. Mezger, M. Morris, and J. Lacy for helpful comments. Professor H. van der Laan generously supported the observations with the SHARP camera at the NTT. P. Duhoux wrote a large fraction of the SHARP software.

REFERENCES

- Allen, D. A. 1987, in AIP Conf. Proc. 155, The Galactic Center, ed. D. Backer (New York: AIP), 1
- Allen, D. A., Hyland, A. R., & Hillier, D. J. 1990, MNRAS, 244, 706
- Bailey, M. E. 1980, MNRAS, 190, 217
- Becklin, E., Dinerstein, H., Gatley, I., Werner, M. W., & Jones, B. 1987, in AIP Conf. Proc. 155, The Galactic Center, ed. D. Backer (New York: AIP), 162
- Becklin, E. E., & Neugebauer, G. 1968, ApJ, 151, 145
- . 1975, ApJ, 200, L71
- Christou, J. C. 1991, Exp. Astron. 2, 27
- DePoy, D. L., & Sharp, N. A. 1991, AJ, 101, 1324
- Eckart, A., & Duhoux, P. R. M. 1990, in Astrophysics with Infrared Arrays, ed. R. Elston (ASP Conf. Ser. 14), 336
- Eckart, A., Genzel, R., Krabbe, A., Hofmann, R., van der Werf, P. P., & Drapatz, S. 1992, Nature, 335, 526
- Forrest, W. J., Shure, M. A., Pipher, J. L., & Woodward, C. E. 1987, in AIP Conf. Proc. 155, The Galactic Center, ed. D. C. Backer (New York: AIP), 153
- Gatley, I., Joyce, R., Fowler, A., DePoy, D., & Probst, R. 1989, in The Center of the Galaxy, ed. M. Morris (Dordrecht: Kluwer), 361
- Geballe, T. R., Krisciunas, K., Bailey, J. A., & Wade, R. 1991, ApJ, 370, L73
- Genzel, R. 1989, in The Center of the Galaxy, ed. M. Morris (Dordrecht: Kluwer), 393
- Goodman, J., & Lee, H. M. 1989, ApJ, 337, 84
- Hofmann, R., Blietz, M., Duhoux, P., Eckart, A., Krabbe, A., & Rotaciuc, V. 1993, in Progress in Telescope and Instrumentation Technologies, ed. M. H. Ulrich (ESO Rep. 42), 617
- Jackson, J. M., Geis, N., Genzel, R., Harris, A. I., Madden, S. C., Poglitsch, A., Stacey, G. J., & Townes, C. H. 1993, ApJ, 402, 173
- Knox, K. T. 1976, J. Opt. Soc. Am., 66, 1236
- Krabbe, A., Genzel, R., Drapatz, S., & Rotaciuc, V. 1991, ApJ, 382, L19
- Krabbe, A., et al. 1993, in preparation
- Krenz, T., et al. 1993, in preparation
- Lebofsky, M. J., Rieke, G. H., & Tokunaga, A. T. 1982, ApJ, 263, 736
- Lee, H. M. 1987, ApJ, 319, 771
- . 1990, in Dynamics of Dense Stellar Systems, ed. D. Merritt (Cambridge: Cambridge Univ. Press), 105
- Lucy, L. B. 1974, AJ, 79, 745
- Moneti, A., Glass, I. S., & Moorwood, A. F. M. 1991, Mem. Soc. Astron. Ital., 62, 755
- Morris, M. 1993, preprint
- Murphy, B. W., Cohn, H. N., & Durison, R. H. 1988, in Dynamics of Dense Stellar Systems, ed. D. Merritt (Cambridge: Cambridge Univ. Press), 97
- Okuda, H., et al. 1990, in The Center of the Galaxy, ed. M. Morris (Dordrecht: Kluwer), 281
- Ozernoy, L. M. 1987, in AIP Conf. Proc. 155, The Galactic Center, ed. D. Backer (New York: AIP), 181
- Phinney, E. S. 1989, in The Center of the Galaxy, ed. M. Morris (Dordrecht: Kluwer), 543
- Rieke, G. H., & Lebofsky, M. J. 1982, in The Galactic Center, ed. G. R. Riegler & R. D. Blandford (New York: AIP), 194
- Rieke, G. H., Rieke, M. J., & Paul, A. E. 1989, ApJ, 336, 752
- Rosa, M. R., Zinnecker, H., Moneti, A., & Melnick, J. 1992, A&A, 257, 515
- Sanders, R. H. 1992, Nature, 359, 131
- Sellgren, K., Hall, D. N. B., Kleinmann, S. G., & Scoville, N. Z. 1987, ApJ, 317, 881
- Sellgren, K., McGinn, M. T., Becklin, E. E., & Hall, D. N. B. 1990, ApJ, 359, 112
- Serabyn, E., Carlstrom, J. E., & Scoville, N. 1992, ApJ, 401, L87
- Simon, M., Chen, W. P., Forrest, W. J., Garnett, J. D., Longmore, A. J., Gauer, T., & Dixon, R. I. 1990a, ApJ, 360, 95
- Simons, D. A., Hodapp, K. W., & Becklin, E. E. 1990b, ApJ, 360, 106
- Tollestrup, E. V., Capps, R. W., & Becklin, E. E. 1989, AJ, 98, 204
- Yusef-Zadeh, F., & Melia, F. 1992, ApJ, 385, L41
- Zylka, R., Mezger, P. G., & Lesch, J. 1992, A&A, 261, 119